Aalborg Universitet

Lifetime analysis of two commercial PV converters using multi-year degradation modelling

Fogsgaard, Martin Bendix; Zhang, Yi; Bahman, Amir Sajjad; Iannuzzo, Francesco; Blaabjerg, Frede

Published in:
e-Prime - Advances in Electrical Engineering, Electronics and Energy

DOI (link to publication from Publisher):
10.1016/j.prime.2023.100205

Creative Commons License
CC BY-NC-ND 4.0

Publication date:
2023

Document Version
Publisher's PDF, also known as Version of record

Link to publication from Aalborg University

Citation for published version (APA):
Fogsgaard, M. B., Zhang, Y., Bahman, A. S., Iannuzzo, F., & Blaabjerg, F. (2023). Lifetime analysis of two commercial PV converters using multi-year degradation modelling. *e-Prime - Advances in Electrical Engineering, Electronics and Energy*, *5*, [100205]. https://doi.org/10.1016/j.prime.2023.100205

General rights
Copyright and moral rights for the publications made accessible in the public portal are retained by the authors and/or other copyright owners and it is a condition of accessing publications that users recognise and abide by the legal requirements associated with these rights.

- Users may download and print one copy of any publication from the public portal for the purpose of private study or research.
- You may not further distribute the material or use it for any profit-making activity or commercial gain
- You may freely distribute the URL identifying the publication in the public portal -

Take down policy
If you believe that this document breaches copyright please contact us at vbn@aub.aau.dk providing details, and we will remove access to the work immediately and investigate your claim.

e-Prime - Advances in Electrical Engineering, Electronics and Energy 5 (2023) 100205

Contents lists available at ScienceDirect

e-Prime - Advances in Electrical Engineering, Electronics and Energy

journal homepage: www.elsevier.com/locate/prime

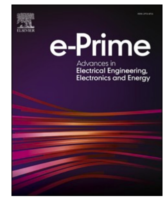

Lifetime analysis of two commercial PV converters using multi-year degradation modelling

Martin Bendix Fogsgaard *, Yi Zhang, Amir Sajjad Bahman, Francesco Iannuzzo, Frede Blaabjerg

Department of Energy Technology, Aalborg University, Aalborg, Denmark

ARTICLE INFO

Keywords:
Reliability
Power electronics
PV Converters
Reliability prediction
Degradation feedback
Degradation based end-of-life

ABSTRACT

This paper presents a practical method to perform multi-year degradation modeling for power electronics reliability analysis. It will present how to combine a PV mission profile simplification method with a parameter degradation feedback mechanism. The overall method is presented, along with how to characterize the parameters for the method from experimental results. The method and the characterization method are demonstrated against simulated wear-out curves based on experimental lifetime tests. The whole workflow is applied to analyze two commercial PV generator systems in order to compare the inclusion and exclusion of the degradation feedback on lifetime prediction. All model parameters are shown in the paper, and the used mission profiles will be published available online.

1. Introduction

Power electronics make up an ever-increasing part of the modern power grid e.g. with the increased installation of renewable energy sources [1] and it is an important technology to help to fight Global Warming [2].

Photovoltaic (PV) generator systems use power electronics both in the general operation of power point tracking and may contain power converters to boost the output voltage and/or convert to alternating current in order to connect to the power grid.

When a PV generator system is planned, the reliability of the system is of great importance both for commercial and residential systems [3].

The reliability analysis is an important tool to determine whether the system is economically viable and it gives insight into the risk of system failure over time. A common reliability analysis workflow for a power electronic system is seen in Fig. 1.

The workflow seen in Fig. 1 and variations thereof are used in numerous papers such as [4–9]. All of these papers use the workflow or adaptations, e.g. [9] combines it with artificial intelligence to find the optimum design parameters for system reliability.

The planned location of a PV system is taken into account via a mission profile describing the operating conditions caused by the solar power and ambient temperature. An example of a mission profile can be seen in Fig. 2.

The most time-consuming part of the mentioned workflow is the simulation of the system behaviour over an entire year. However, in some cases, the simulation time can be reduced [10–13].

Conventionally, some effects are neglected from reliability analysis because of the difficulty of integrating them into the simulation of mechanisms occurring at different timescales. One effect is the degradation of the analyzed components, such as bond-wire lift-off and solder layer de-lamination. Studies such as [14] have found that degradation can have a significant effect on the tested device lifetime and efforts should be made to include these effects in the analysis.

Damage modelling for IGBTs and power electronics in general has been investigated in previous literature such as [15–20].

This forms the basis of what will be investigated in this paper, degradation modeling will be performed on two commercial PV converters and the effect of degradation on lifetime will be evaluated.

2. The simplification method

The simplification procedure of [12] can be used directly in the workflow outlined in Fig. 1 and greatly reduces the computation time of the reliability analysis.

The time reduction is controlled by the user by choosing a number of representative days.

* Corresponding author.
E-mail address: mbf@energy.aau.dk (M.B. Fogsgaard).

https://doi.org/10.1016/j.prime.2023.100205
Received 19 May 2023; Received in revised form 11 June 2023; Accepted 26 June 2023
Available online 3 July 2023
2772-6711/© 2023 The Authors. Published by Elsevier Ltd. This is an open access article under the CC BY-NC-ND license (http://creativecommons.org/licenses/by-nc-nd/4.0/).

2.1. Principle of the method

The method works by replacing the 365-day mission profile with a synthetic, simplified mission profile. The simplified profile is simulated using the original model and afterward, a 365-day junction temperature profile is reconstructed using the simulation results.

The simplification method is performed as a part of the simulation pre-processing and post-processing, this makes the simplification method independent of the simulation model. Comparing Figs. 1 with 3 shows where the pre- and post-processing steps are added, and it can be seen that the modeling step is retained.

In this work, an averaged loss model and thermal network based on reference [21] is used, but other models may be used with the simplification method.

An improved version can be found in [13], the basic principle is the same, but the synthesis methodology is improved in order to remove the dependence on arid climates.

3. Multi-year degradation modelling

The full multi-year degradation modeling workflow is a natural extension of the simplification model of Section 2 and [12]. As the simulation of a single year can be done in seconds, it becomes practical to not only simulate multiple years but also to add parameter evolution as a result of the degrading components and interfaces.

The entire multi-year workflow can be seen in Fig. 4. The first box is the mission profile input containing both power and ambient temperature profiles. The same one-year profile can be repeated for multi-year analysis or a multi-year profile may be used.

The month of the mission profile is simulated as described in Section 2 and [12]. Then the junction temperature profile of that month is evaluated using Rainflow Counting, Palmgren-Miner's Rule and the chosen damage model. The total accumulated damage is linked to each degrading component using the degradation function.

$$d = 1 - (1 - D)^k \tag{1}$$

Where d is degradation, D is the accumulated damage and k is the non-linear degradation shape parameter.

For some degrading components the parameters will change very little during their life and only change near wear-out, for others, the damage and degradation will follow each other almost linearly, and finally some parameters "wear-in" at the beginning of their life and don't change very much for the remainder of the lifetime. This is what Eq. (1) represents with the shape parameter k determining if the link is linear, wear-in, or wear-out.

An example of a degrading parameter could be the electrical resistance of a bond-wire foot. This can be seen in Eq. (2).

$$R(a_i, a_o) \approx \frac{\rho_{Al} l_{bw}}{\pi r^2} + \frac{\rho_{Al} a_i}{\pi r^2} + \frac{\rho_{Al} d_c}{w_f (l_f - a)} \tag{2}$$

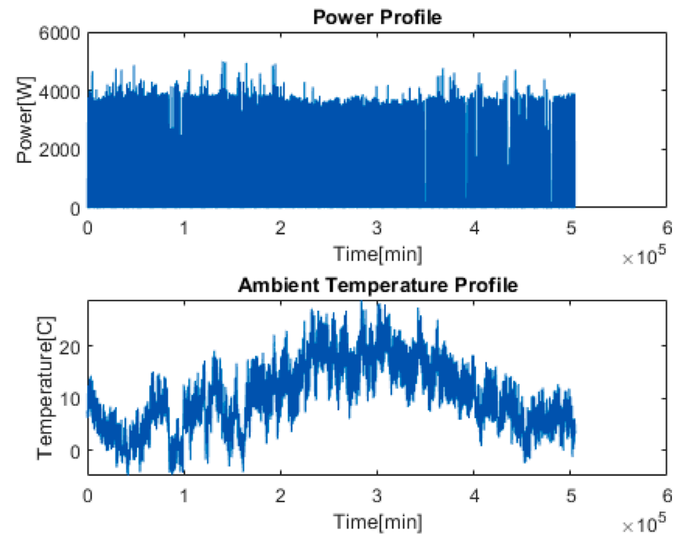

Fig. 2. An example of a mission profile with both power and ambient temperature profiles.

Where R is resistance, ρ_{Al} is resistivity, l_{bw} is bond wire length. d_c is crack thickness. w_f is bond-wire foot width and r is bond wire radius. a_i and a_o are the lengths of cracks propagating from the inner bond wire tip and the outer bond wire tip.

The thermal resistance evolution of the degraded solder layer, which is another degrading parameter, can be calculated similarly.

When the parameter degradation has been calculated, the simulation is continued in the next month in the mission profile. This process is repeated until the degraded parameters have reached their end-of-life threshold, the same way that physical devices are considered worn out when their parameters degrade beyond the end-of-life threshold.

4. Characterisation of parameter based degradation models

The empirical data needed to apply this method is very similar to that conventionally used [22] for non-degradation approaches. Power cycling is conducted and the loading conditions and the number of cycles to failure for each condition are recorded. Additionally, the evolution of each modeled degrading parameter must be recorded for each loading condition. If a simulation of thermal interface wear-out is required, then the evolution of thermal resistance during power cycling must be recorded.

Once the power cycling is completed and the required quantities are recorded, the characterization can be done using a few equations and an optimization algorithm.

First, an initial fitting is made based on the experimental life results. This fitting is based on initial guesses for A, B, C, and k.

Secondly, degradation and damage equations are set up for each

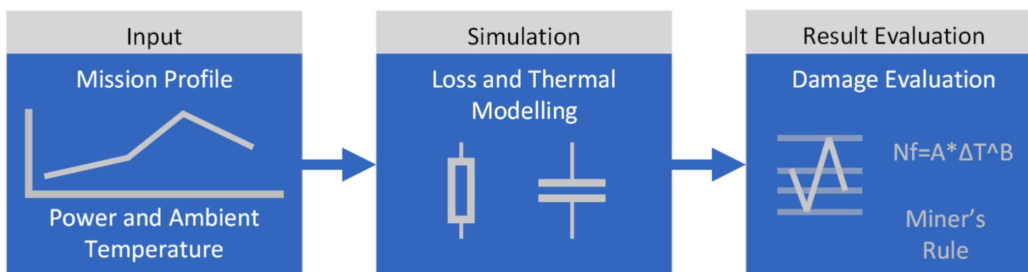

Fig. 1. Commonly used reliability analysis workflow for power electronics. The input to the modeling is a mission profile containing time-series data of the relevant input parameters such as input power and ambient temperature. The input is processed by a behavioral model, such as a loss model and thermal network, to translate the input into a time-series profile of the resulting thermal loading. The loading profile is counted using the Rainflow Counting Algorithm and a damage model along with the Palmgren-Miner's Rule of Linear Damage Accumulation is used to evaluate the damage to the system or component as a result of the input profile.

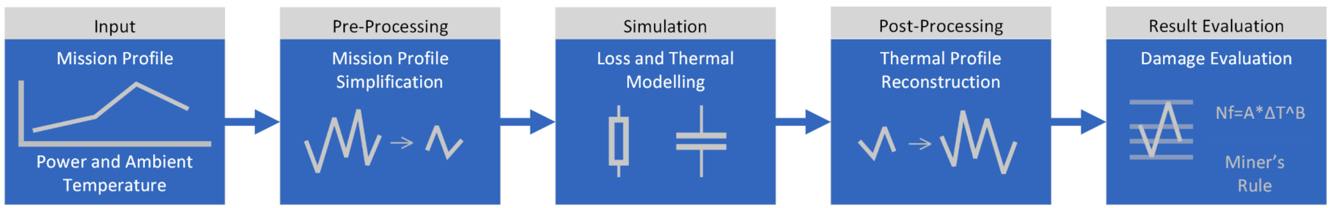

Fig. 3. The pre and post-processing steps in relation to the methodology of Fig. 1.

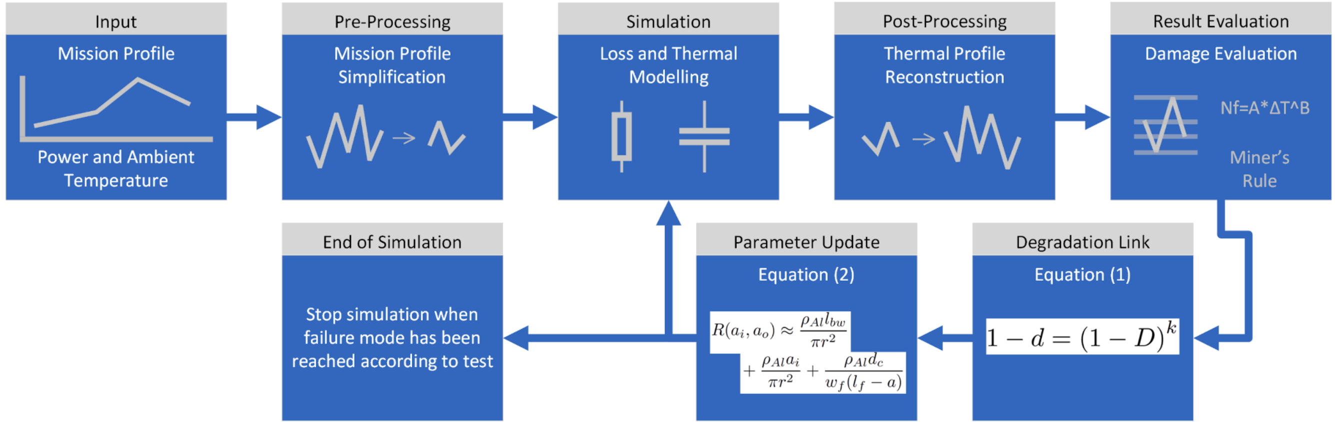

Fig. 4. The overall workflow for multi-year reliability analysis.

degrading parameter. The simulation model is based on the assumption that damage can be considered to be accumulated in discrete steps. As a result, the wear-out curves are split into several steps. For a given step, the junction temperature swing, damage of this step, and total accumulated damage at the last step are known. This allows us to set up the following equations:

$$D^i = \frac{N^i - N^{i-1}}{N_f^i} \tag{3}$$

Where D^i is the damage of the current step, $N^i - N^{i-1}$ is the number of cycles from the previous to this step. N_f^i is the number of cycles to failure for the current loading conditions which can be calculated using Eq. (6) and the A, B, and C fitting parameters. Another damage model can also be used.

$$d^i = 1 - \left(1 - \sum_{j=1}^{i} D^j\right)^k \tag{4}$$

Where d^i is the degradation of the current step, k is the crack shape parameter, and D^j is the damage of the jth step. The stepping procedure can be seen in Fig. 6.

The fitted and experimental degradation evolution are compared to find the error of the fit.

$$RMSE = \sqrt{\left(d_{fitted} - d_{experiment}\right)^2} \tag{5}$$

RMSE is the root mean square error calculated from the fitted(d_{fitted}) and experimental($d_{experimental}$) degradation curves. d_{fitted} is the complete series of all d_is.

Using Eqs. (3) to (5), the damage and degradation equations are linked to the experimental degradation curves, and using an optimization algorithm such as the Newton-Raphson method, the optimal values for A, B, C, and k can be found.

The methodology was followed for six loading conditions for the same power device. The simulated validation curves and experimental reference curves can be seen in Fig. 7. The experimental curves are

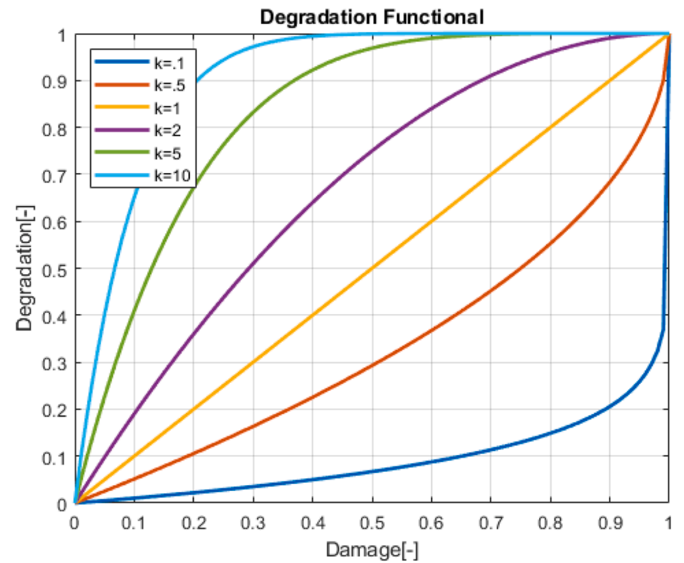

Fig. 5. A comparison of the non-linear coupling of damage and degradation for different shape parameter values as given by Eq. (1). k=1 results in a linear coupling of degradation to damage, $k > 1$ is for wear-in effects, and $k < 1$ is for wear-out degradation.

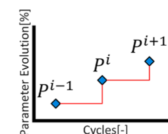

Fig. 6. Degradation points P^{i-1}, P^i and P^{i+1}. The parameter(s) and the degradation is considered to be constant between the cycling steps and it is updated when a new point is reached.

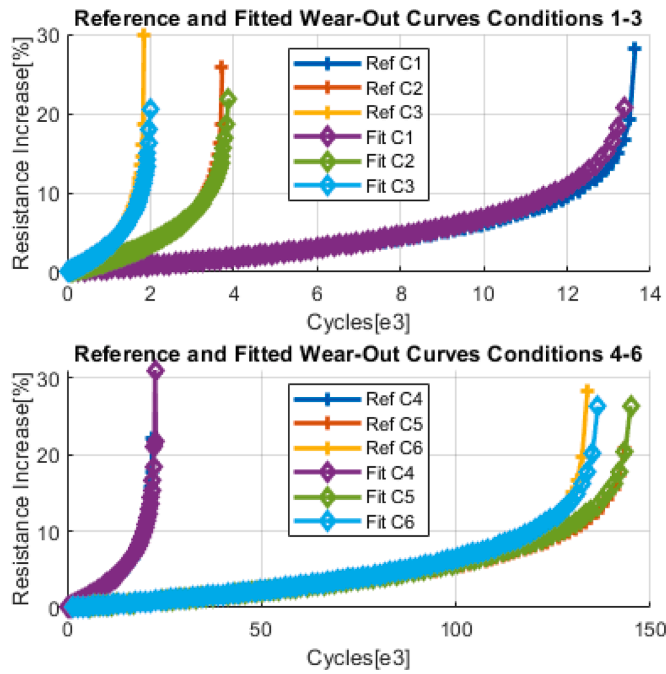

Fig. 7. Simulated reference and fitted degradation curves for six loading conditions from reference [23].

highlighted with crosses and the simulated curves are highlighted with diamonds.

4.1. Example implementation on experimental results

To provide experimental wear-out data to demonstrate the fitting process, DC power cycling was conducted on an IGBT module. The module used is a three-phase FS25R12KT3 module. It was attached to a fixed temperature cooling plate and cycled with 44.3 A current pulses with 5 s on and off time. The evolution of the temperature swings can be seen in blue in Fig. 8.

The wear-out curve was processed using the workflow described in Section 4. The resulting fitted curve was compared to the original curve and the two curves can be seen in Fig. 8.

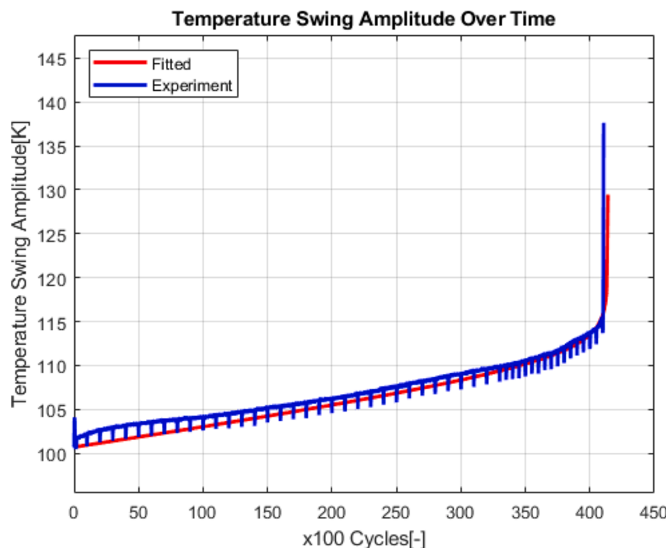

Fig. 8. Experimentally determined temperature evolution(blue) and fitted curve(red). (For interpretation of the references to colour in this figure legend, the reader is referred to the web version of this article.)

5. Case study on commercial inverters

The proposed methodology presented in previous sections is applied to two commercial PV inverters to compare them with the enabled analyses and to demonstrate the possible results of the method.

5.1. System 1

The analysed system is an Impedance-source-based PV microinverter from UBIK Solutions [24]. It is a two-stage system with a Quasi-Z-Source series resonant DC-DC converter and a single phase grid-tied inverter with output filter. More details on the operation of the topology can be found in literature [25]. The topology can be seen in Fig. 9.

As an overall reliability analysis has already been performed on this system [27], this work will focus on the effect of including the degradation in the inverter subsystem.

The inverter uses four SCT2120AF MOSFETs, where the electrical parameters for operation and loss modeling can be found in the datasheet [28].

The thermal parameters for both the MOSFETs and for the path from case to ambient can be extracted from the previous reliability analysis [27]. The parameters were extracted in Foster network form and it can be seen in Table 1.

The reliability model for the bond-wires will be that determined experimentally in [29]. It is assumed that these parameters, while not experimentally determined for the exact transistors used, will give an accurate comparison between the inclusion and exclusion of degradation feedback in the analysis. The exact values for the model parameters are $\alpha = 5{\cdot}10^{11}$ and $m = 5.3$

The degradation shape parameter for the solder layer was characterised from the experimental results of [30] and was found to be $k = 0.1445$. The damage model for the solder layer and the model parameters used will be those determined experimentally in [17].

$$N_f = A\Delta T_j^B e^{\left(\frac{C}{T_{mean}+273}\right)} \tag{6}$$

Where N_f is the number of cycles to failure, ΔT_j is the temperature swing, T_{mean} is the mean temperature. A, B and C are model parameters with the values of $A = 97.2231$, $B = -3.1292$ and $C = 7.1667e+03$ [17].

5.2. System 2

The second studied system is a Danfoss TLX PRO+ system consisting of three parallel DC/DC boost converters and a three-phase Neutral-Point-Clamped inverter [31]. See the topology in Fig. 10.

The actual power semiconductors of the system are unknown to these authors, so the thermal parameters and damage model parameters from another known system will be used [21]. These parameters are seen in Table 2.

The damage model used is:

$$N_f = A\left(\Delta T_j\right)^{\beta_1} \cdot e^{\frac{\beta_2}{T_{j,min}+273}} t_{on}^{\beta_3} I_B^{\beta_4} V_C^{\beta_5} D^{\beta_6} \tag{7}$$

Where N_f is the number of cycles to failure, ΔT_j is the temperature swing, $T_{j,min}$ is the minimum temperature of the cycle and t_{on} is the cycle period. The fitting parameters are $A = 9.37{\cdot}10^{14}$, $\beta_1 = -4.416$, $\beta_2 = 1285$, $\beta_3 = -0.463$, $\beta_4 = -0.716$, $\beta_5 = -0.761$ and $\beta_6 = -0.5$. The system parameters are $I_B = 12.5$, $V_C = 15$, and $D = 30$.

The thermal case to ambient parameters for system 2 were extracted from a fluid flow simulation of the heatsink during operation. The geometry of the real system was simplified and built in COMSOL Multiphysics, and simulated similarly to the process found in the application gallery [32]. The thermal parameters in Foster network form can be found in Table 2.

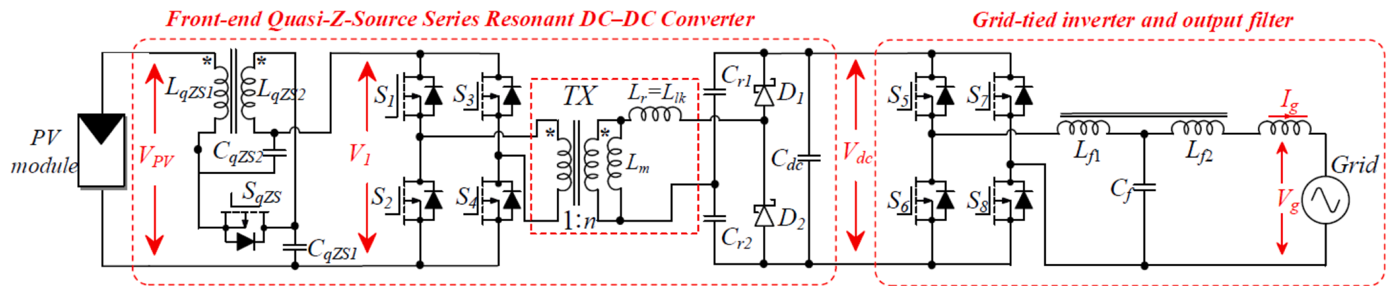

Fig. 9. The entire PV generator system of [26]. The consists of a DC/DC converter stage and an inverter stage with output filter. The damage and degradation of S_5 is the focus point of this paper, but the same analysis can be conducted for all semiconductors in the system.

Table 1
Thermal parameters from [27] and [28] in Foster network form.

Level	Resistance	Capacitance
Junction-Case 1	0.04197 [K/W]	0.001471 [J/K]
Junction-Case 2	0.2677 [K/W]	0.06857 [J/K]
Junction-Case 3	0.3778 [K/W]	0.006633 [J/K]
Case-Ambient	1.759 [K/W]	2774 [J/K]

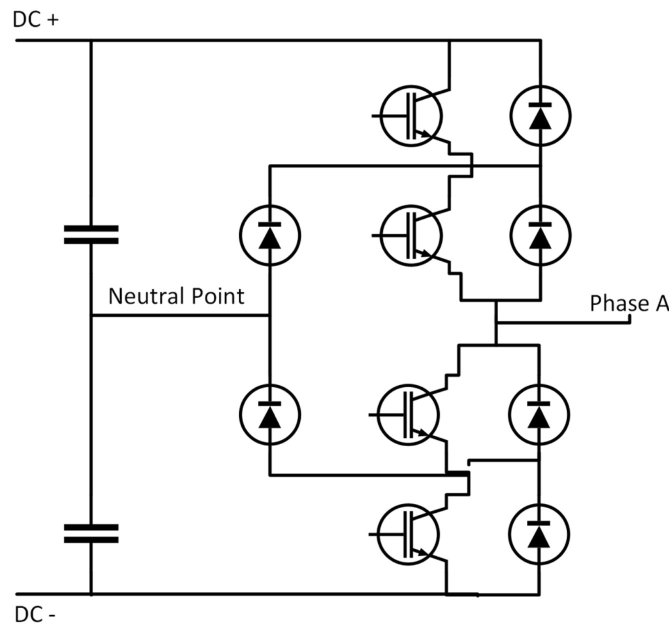

Fig. 10. One leg of the NPC inverter system of the Danfoss TLX PRO+ (the other two identical legs, the L-filter, and three parallel input boost converters are not pictured).

Table 2
Thermal parameters of the Danfoss system in Foster network form.

Level	Resistance	Capacitance
Junction-Case 1	0.0324 [K/W] [21]	0.3086 [J/K] [21]
Junction-Case 2	0.1782 [K/W] [21]	0.1122 [J/K] [21]
Junction-Case 3	0.1728 [K/W] [21]	0.2894 [J/K] [21]
Junction-Case 4	0.1566 [K/W] [21]	0.6386 [J/K] [21]
Case-Ambient 1	0.0202 [K/W]	138.4 [J/K]
Case-Ambient 2	0.0191 [K/W]	865 [J/K]
Case-Ambient 3	0.0415 [K/W]	61.7 [J/K]

5.3. Mission profiles

Five real mission profiles from different locations will be used in the analysis. The locations are Arizona, Colorado, Denmark, Sacramento, and Spain.

The mission profiles contain the irradiance and ambient temperature profiles for an entire year, sampled at a 1-minute resolution.

The profiles have previously been used in [12] and [13], and the Denmark profile was also used in [27]. As profiles sampled at a resolution with less than an hour per sample be difficult to come by, the profiles will be made available at the publication of the paper [33].

6. Study case: Commercial converter 1

The UBIK system was modeled with the parameters of Section 5.1 and subjected to all of the 5 mission profiles of Section 5.3. The temperature swing, solder damage, and thermal resistance evolution can be seen in Fig. 11 which is initially linear, but as the resistance rises above a certain threshold the temperature swing will begin to increase noticeably. This in turn will increase the damage accumulation, which will increase the thermal resistance even more. This positive feedback mechanism caused by degradation is a major factor in the final lifetime prediction [14]. The projected lifetime from the period of linear damage

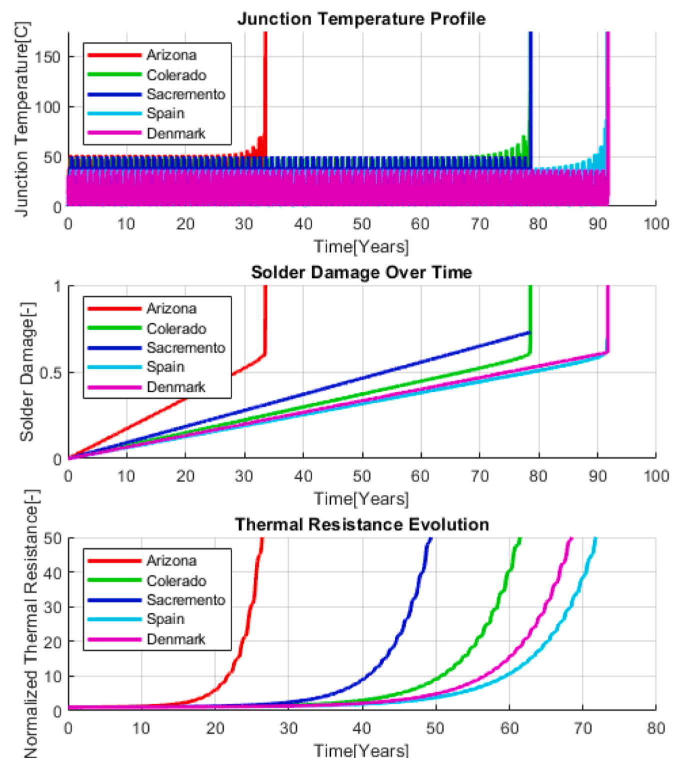

Fig. 11. Damage and degradation evolution of Converter 1. The damage increases linearly for most of the life of these systems, but at certain points, the thermal run-away mechanism kicks in because of the degradation feedback mechanism.

accumulation was calculated and Fig. 12 shows that the positive feedback mechanism reduces lifetime by 20–60+ years.

The UBIK is a microinverter system wrapped in a plastic case. As such, the relative thermal resistance from junction to case is much lower than the resistance from case to ambient. This is the reason why the thermal resistance of the solder layer needs to rise to 40–60 times the original value before the temperature swing in Fig. 11 starts to increase.

7. Study case: Commercial converter 2

The lifetime evolution of the bond-wire and solder layer damage and the evolution of the thermal resistance can be seen in Fig. 13. In the figure, the thermal resistance is normalized according to the initial value, and a final value of “50” corresponds with a thermal resistance that is 50 times the initial value. The thermal resistance evolution of the Danfoss system is highly non-linear and exhibits an exponential increase in the final stage of life.

In Fig. 13 the damage evolution of the bond-wire and solder layers increase linearly for the majority of the lifetime of the system, but near the end of life the device enters a phase with abnormal operation and a rapid increase of solder layer damage. In Fig. 13 the junction temperature profiles during the lifetime of the systems can be seen. Here it can be seen that the five systems had a greatly increased maximum temperature during the final period of their lifetime.

The Converter 1 system experienced the same positive feedback phenomenon as the Converter 2 system, and the phenomenon was also a strong factor in determining the final lifetime. The initial linear damage rate was extrapolated to compare the lifetime without and with degradation. The feedback mechanism was found to reduce lifetime by more than 50% compared to the linearly projected life as can be seen in Fig. 14.

7.1. Impact of degradation shape parameter

The range of k for solder layer delamination and the evolution of the thermal resistance was approximated from literature to find sample sets. These can be seen in Table 3.

To show the impact of these parameters and the behaviour of the five

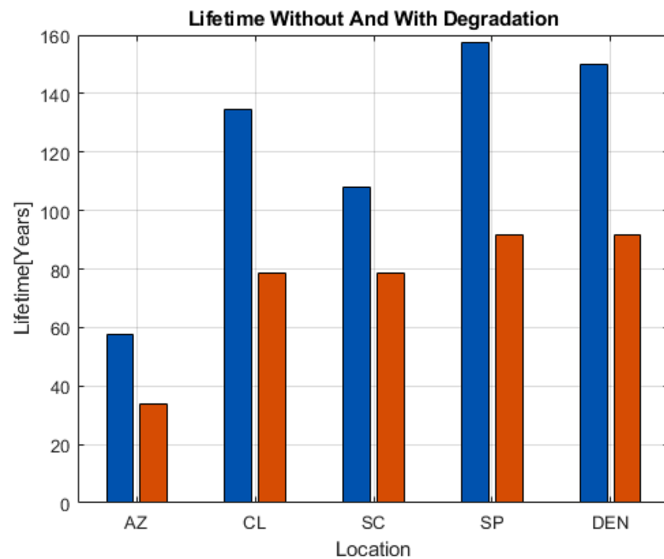

Fig. 12. The effect of damage feedback on the simulated lifetime of Converter 1 can be seen by comparing the blue and red lifetimes at each location. The red lifetimes were found using the proposed method of this paper and the blue lifetimes were found by repeating the yearly damage caused by an undegrading system. (For interpretation of the references to colour in this figure legend, the reader is referred to the web version of this article.)

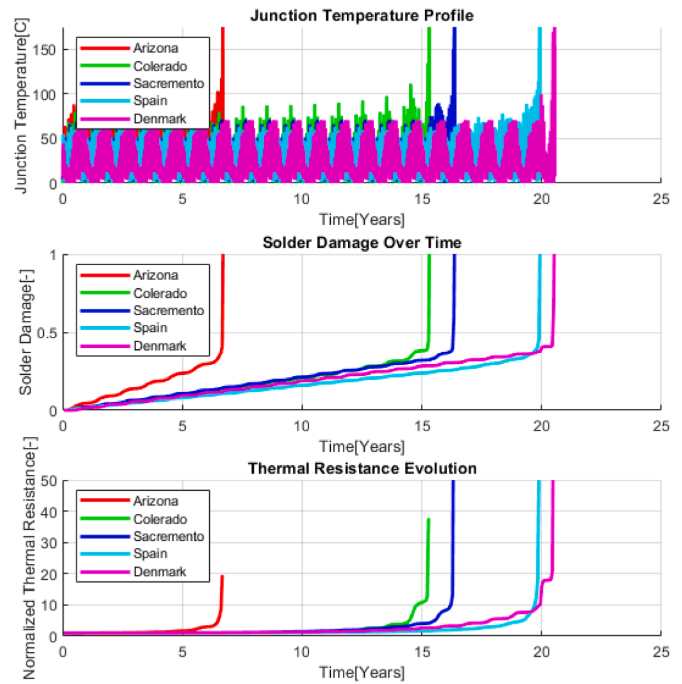

Fig. 13. The damage and degradation evolution of Converter 2 for different mission profiles.

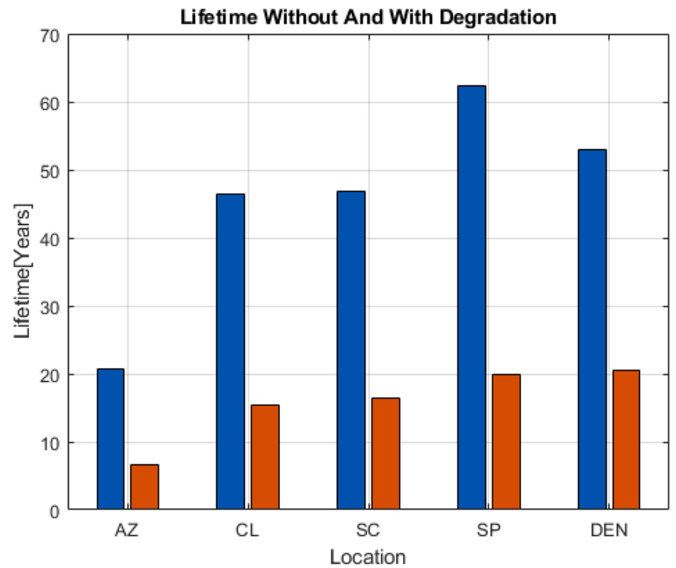

Fig. 14. Lifetime prediction without(blue) and with degradation(red) of Converter 2. (For interpretation of the references to colour in this figure legend, the reader is referred to the web version of this article.)

Table 3
Degradation parameters from literature.

Parameter	a	b	k	
Case 1	0.02979	1.000111	4.278	[30]
Case 2	0.0002544	0.9877	3.902	[34]
Case 3	0.01764	1.08498	0.8485	[34]
Case 4	0.000512	1.035	5.622	[17]
Case 5	0.2152	0.7848	0.06	Experiment

sample sets in Table 3, they were compared using the simulation procedure of Fig. 4 and the Arizona mission profile. The behaviour can be seen in Fig. 15.

To investigate the raw impact of the k parameter, the simulation was repeated with the Converter 2 system and the Arizona profile, only altering the k parameter from 1 (the linear case) to 5.5 (the maximum value of k from Table 3). As seen in Fig. 5, the higher the k value, the earlier the degradation will increase to 1. As a result, the higher the k value, the earlier the positive feedback mechanism will be activated, leading to a shorter lifetime for higher k values. This inverse proportionality can be seen in Fig. 16 where higher k values will enter faster into abnormal operation.

8. Conclusion

This paper has presented an analysis of the lifetime of two commercial PV systems considering the degradation of the thermal resistance of the solder layer. The degradation modelling was presented in detail, along with how to characterize it.

Degradation-based lifetime modelling offers two advantages compared to the conventional methodology. First, the degradation causes a change in the behaviour of the system, which in turn may cause a feedback loop of the damage which is accelerating the wear-out and thereby shorten the lifetime.

Secondly, modelling the degradation enables a parametrically defined end-of-life, where failure can be defined as 10% increase in Vce (on), 20% increase in thermal resistance, 50% increase in power loss, or an increase in any other damage-sensitive parameter.

Thanks to the simplification method of [13], the presented method

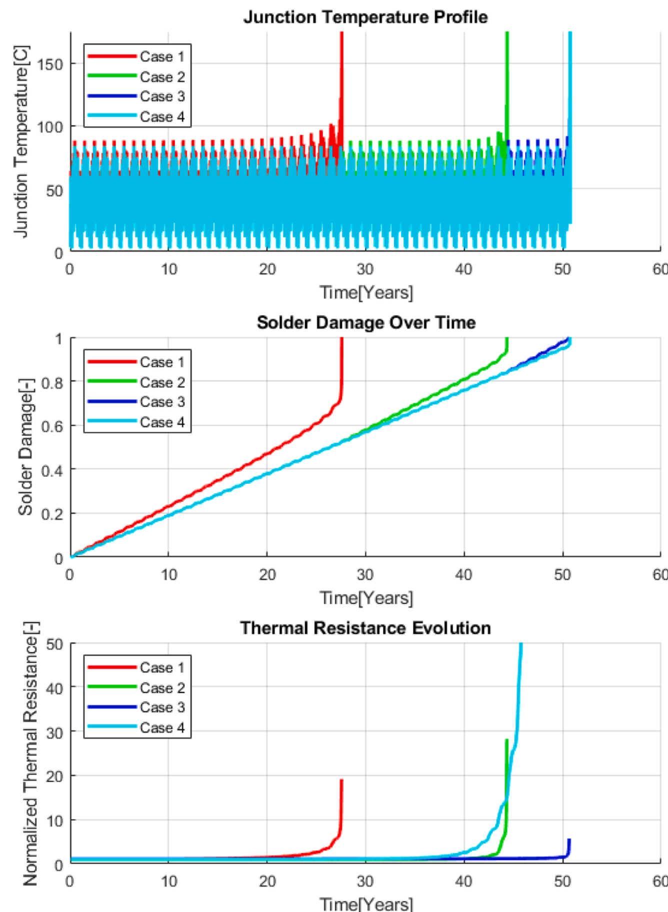

Fig. 15. Lifetime results for the 5 different sets of degradation and resistance evolution parameters.

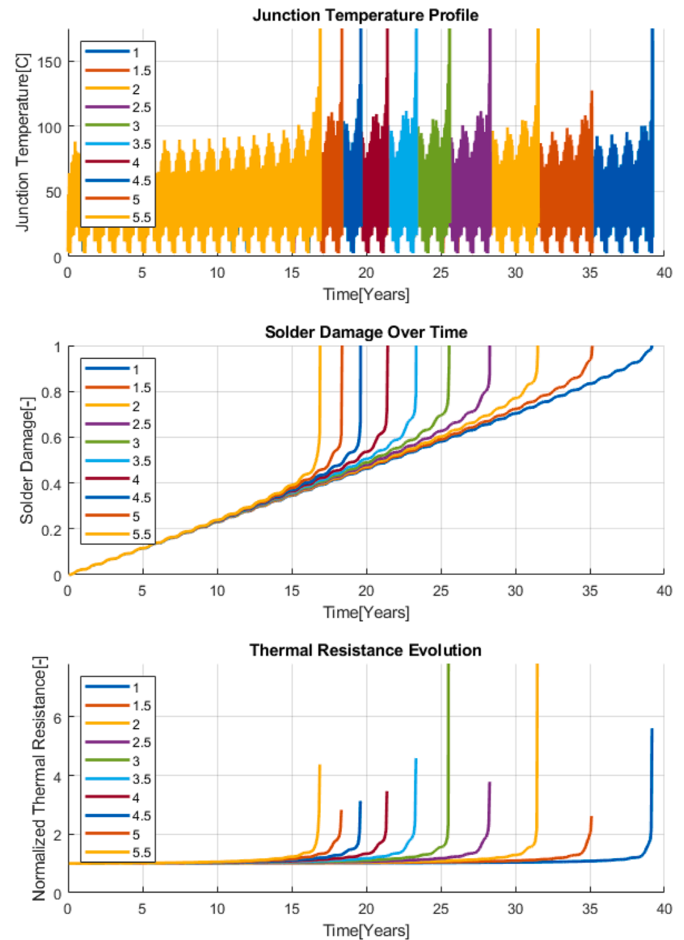

Fig. 16. Lifetime results for a parameter sweep of k from 1 to 5.5. Converter 2 and Arizona profile.

including degradation feedback is fast enough to be practically used. The total time needed to fit the 6 degradation curves of Fig. 7 was 340 s, and the total time to simulate the validation curves was 330 s.

The method was demonstrated using two system cases where it was found that the positive feedback mechanism strongly affect the system lifetime prediction for both systems as it was expected in [14].

The relative impact of the degradation shape parameter k was investigated using a parameter sweep of both k and of different sets of degradation parameters from literature. The higher the k is, the larger the impact of degradation will be. The k parameter for a degrading quantity can be used as an indicator for the impact of the degradation on that quantity. It can be used to decide whether the degradation of that parameter needs to be included in the modelling.

Declaration of Competing Interest

The authors declare that they have no known competing financial interests or personal relationships that could have appeared to influence the work reported in this paper.

The authors declare the following financial interests/personal relationships which may be considered as potential competing interests:

Martin Bendix Fogsgaard reports financial support was provided by Villum Foundation.

Data availability

Data will be made available on request.

Acknowledgments

This research is funded by Villum Fonden under the REPEPS Project.

References

[1] Hitachi Energy, Power electronics: revolutionizing the worlds future energy systems[Online]. Available: https://www.hitachienergy.com/news/perspectives/2021/08/power-electronics-revolutionizing-the-world-s-future-energy-systems.
[2] B. Bose, Global warming: energy, environmental pollution, and the impact of power electronics, IEEE Ind. Electron. Mag. 4 (1) (2010) 6–17.
[3] J. Falck, C. Felgemacher, A. Rojko, M. Liserre, P. Zacharias, Reliability of power electronic systems: an industry perspective, IEEE Ind. Electron. Mag. 12 (2) (2018) 24–35, https://doi.org/10.1109/MIE.2018.2825481.
[4] K. Ma, H. Wang, F. Blaabjerg, New approaches to reliability assessment: using physics-of-failure for prediction and design in power electronics systems, IEEE Power Electron. Mag. 3 (4) (2016) 28–41, https://doi.org/10.1109/MPEL.2016.2615277.
[5] M. Musallam, C. Yin, C. Bailey, M. Johnson, Mission profile-based reliability design and real-time life consumption estimation in power electronics, IEEE Trans. Power Electron. 30 (5) (2015) 2601–2613, https://doi.org/10.1109/TPEL.2014.2358555.
[6] A. Sangwongwanich, Y. Yang, D. Sera, F. Blaabjerg, Lifetime evaluation of grid-connected PV inverters considering panel degradation rates and installation sites, IEEE Trans. Power Electron. 33 (2018) 1125–1236, https://doi.org/10.1109/TPEL.2017.2678169.
[7] D. Zhou, H. Wang, F. Blaabjerg, Mission profile based system-level reliability analysis of DC/DC converters for a backup power application, IEEE Trans. Power Electron. 33 (2018) 8030–8039, https://doi.org/10.1109/TPEL.2017.2769161.
[8] K. Ma, U.M. Choi, F. Blaabjerg, Prediction and validation of wear-out reliability metrics for power semiconductor devices with mission profiles in motor drive application, IEEE Trans. Power Electron. 33 (2018) 9843–9853, https://doi.org/10.1109/TPEL.2018.2798585.
[9] T. Dragicevic, P. Wheeler, F. Blaabjerg, Artificial intelligence aided automated design for reliability of power electronic systems, IEEE Trans. Power Electron. 34 (8) (2019) 7161–7171, https://doi.org/10.1109/TPEL.2018.2883947.
[10] A.S. Bahman, F. Iannuzzo, F. Blaabjerg, Mission-profile-based stress analysis of bond-wires in SiC power modules, Microelectron. Reliab. 64 (2016) 419–424, https://doi.org/10.1016/j.microrel.2016.07.102.
[11] L. Ceccarelli, A.S. Bahman, F. Iannuzzo, F. Blaabjerg, A fast electro-thermal co-simulation modeling approach for SiC power MOSFETs. Conference Proceedings - IEEE Applied Power Electronics Conference and Exposition - APEC, 2017, pp. 966–973, https://doi.org/10.1109/APEC.2017.7930813.
[12] M. Fogsgaard, A. Bahman, F. Iannuzzo, F. Blaabjerg, PV mission profile simplification method for power devices subjected to arid climates, Microelectron. Reliab. 126 (2021), https://doi.org/10.1016/j.microrel.2021.114328.
[13] M.B. Fogsgaard, A.S. Bahman, F. Iannuzzo, F. Blaabjerg, Mission profile simplification method for reliability analysis of PV converters, Microelectron. Reliab. (2022) 114651, https://doi.org/10.1016/j.microrel.2022.114651.https://www.sciencedirect.com/science/article/pii/S0026271422001755
[14] H. Luo, N. Baker, F. Iannuzzo, F. Blaabjerg, Die degradation effect on aging rate in accelerated cycling tests of SiC power MOSFET modules, Microelectronics Reliability 76-77 (2017) 415–419, https://doi.org/10.1016/j.microrel.2017.07.004.
[15] R.W. Erickson, D. Maksimović, Fundamentals of Power Electronics, Springer New York, NY, 2001, https://doi.org/10.1007/b100747.ISBN 978-1-4757-0559-1
[16] A. Hanif, Y. Yu, D. Devoto, F. Khan, A comprehensive review toward the state-of-the-art in failure and lifetime predictions of power electronic devices, IEEE Trans. Power Electron. 34 (5) (2019) 4729–4746, https://doi.org/10.1109/TPEL.2018.2860587.
[17] B. Gao, F. Yang, M. Chen, Y. Chen, W. Lai, C. Liu, Thermal lifetime estimation method of IGBT module considering solder fatigue damage feedback loop, Microelectron. Reliab. 82 (2018) 51–61, https://doi.org/10.1016/j.microrel.2017.12.046.
[18] S. Peyghami, H. Wang, P. Davari, F. Blaabjerg, Mission-profile-based system-level reliability analysis in DC microgrids, IEEE Trans. Ind. Appl. 55 (5) (2019) 5055–5067, https://doi.org/10.1109/TIA.2019.2920470.
[19] V.N. Le, L. Benabou, Q.B. Tao, V. Etgens, Modeling of intergranular thermal fatigue cracking of a lead-free solder joint in a power electronic module, Int. J. Solids Struct. 106-107 (2017) 1–12, https://doi.org/10.1016/j.ijsolstr.2016.12.003.
[20] L. Yang, P.A. Agyakwa, C.M. Johnson, Physics-of-failure lifetime prediction models for wire bond interconnects in power electronic modules, IEEE Trans. Device Mater. Reliab. 13 (2013).
[21] A. Sangwongwanich, H. Wang, F. Blaabjerg, Reduced-order thermal modeling for photovoltaic inverters considering mission profile dynamics reduced-order thermal modeling for photovoltaic inverters considering mission profile dynamics, IEEE Open J. Power Electron. 1 (2020) 407–419.
[22] R. Bayerer, T. Herrmann, T. Licht, J. Lutz, M. Feller, Model for power cycling lifetime of IGBT modules - various factors influencing lifetime. 5th International Conference on Integrated Power Systems (CIPS), 2008, pp. 1–6.
[23] A. Otto, S. Rzepka, B. Wunderle, Investigation of active power cycling combined with passive thermal cycles on discrete power electronic devices, J. Electron. Packag. (2019).
[24] S.I. Foundation, Ubik s350 optiverter, [Online]. Available: https://solarimpulse.com/solutions-explorer/ubik-s350-optiverter.
[25] D. Vinnikov, A. Chub, E. Liivik, I. Roasto, High-performance quasi-z-source series resonant DC–DC converter for photovoltaic module-level power electronics applications, IEEE Trans. Power Electron. 32 (5) (2017) 3634–3650, https://doi.org/10.1109/TPEL.2016.2591726.
[26] Y. Shen, H. Wang, Z. Shen, Y. Yang, F. Blaabjerg, A 1-MHz series resonant DC–DC converter with a dual-Mode rectifier for PV microinverters, IEEE Trans. Power Electron. 34 (7) (2019) 6544–6564.
[27] Y. Shen, A. Chub, H. Wang, D. Vinnikov, E. Liivik, F. Blaabjerg, Wear-out failure analysis of an impedance-source PV microinverter based on system-level electrothermal modeling, IEEE Trans. Ind. Electron. 66 (5) (2019) 3914–3927, https://doi.org/10.1109/TIE.2018.2831643.
[28] ROHM Semiconductor, Sct2120af, [Online]. Available: https://eu.mouser.com/datasheet/2/348/sct2120af_e-1871870.pdf.
[29] A. Testa, S. De Caro, S. Russo, A reliability model for power MOSFETS working in avalanche mode based on an experimental temperature distribution analysis, IEEE Trans. Power Electron. 27 (6) (2012) 3093–3100, https://doi.org/10.1109/TPEL.2011.2177279.
[30] Y. Jia, Y. Huang, F. Xiao, H. Deng, Y. Duan, F. Iannuzzo, Impact of solder degradation on VCE of IGBT module: experiments and modeling, IEEE J. Emerg. Sel. Top. Power Electron. 10 (4) (2022) 4536–4545, https://doi.org/10.1109/JESTPE.2019.2928478.
[31] Danfoss, Tlx-inverterserien, fra 6–15 kw, trefasede invertere uden transformator, [Online]. Available: https://co2pro.dk/wp-content/uploads/2018/03/Danfoss_TLX_datablad_DK.pdf.
[32] COMSOL Multiphysics, Heat sink, [online]. Available: https://www.comsol.com/model/heat-sink-8574.
[33] Aalborg University, Aau person profile: Martin bendix fogsgaard, [Online]. Available: https://vbn.aau.dk/da/persons/135365.
[34] W. Lai, M. Chen, L. Ran, S. Xu, N. Jiang, X. Wang, O. Alatise, P. Mawby, Experimental investigation on the effects of narrow junction temperature cycles on die-Attach solder layer in an IGBT module, IEEE Trans. Power Electron. 32 (2) (2017) 1431–1441, https://doi.org/10.1109/TPEL.2016.2546944.

Martin Bendix Fogsgaard is finishing his PhD at the Center of Reliable Power Electronics (CORPE), Aalborg University, Denmark. His research interests include reliability and modelling of power electronic systems and components. He is currently employed at hydrogen fuel cell manufacturer Ballard Power Systems Europe as a Reliability Specialist.

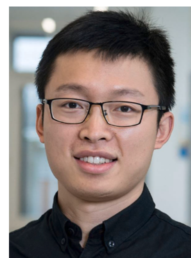

Yi Zhang received the BS and MS degrees from Harbin Institute of Technology, China, in 2014 and 2016, respectively, and the PhD degree from Aalborg University, Denmark, in 2020. All degrees are in electrical engineering. He is currently an assistant professor with Aalborg University, Denmark. During 2020–2023, he was affiliated with multiple institutions as a postdoctoral researcher with the support of the Danish Research Council for Independent Research, including RWTH-Aachen University, Germany, Swiss Federal Institute of Technology Lausanne, Switzerland, and Massachusetts Institute of Technology, USA. He was also a visiting scholar with Georgia Institute of Technology, USA, in 2018. His research interests include the reliability of power electronics. Dr. Zhang received the First Place Prize Paper Award of the IEEE Transactions on Power Electronics in 2021, and the IEEE Power Electronics Society PhD Thesis Talk Award Winner in 2020.

Amir Sajjad Bahman is currently an Associate Professor at the Center of Reliable Power Electronics (CORPE), Aalborg University, Denmark. His research interests include electro-thermo-mechanical modelling, packaging and reliability of power electronic systems and components. Dr. Bahman received the BSc from Iran University of Science and Technology, in 2008, the MSc from Chalmers University of Technology, Sweden in 2011 and the PhD from Aalborg University, Denmark, in 2015 all in electrical engineering. He was a Visiting Scholar in the Department of Electrical Engineering, University of Arkansas, USA, in 2014. Moreover, he was with Danfoss Silicon Power, Germany in 2014 as the Thermal Design Engineer. Dr. Bahman is a senior member of the IEEE and currently serves as an Associate Editor for the IEEE the IEEE Transactions on Transportation Electrification, and Elsevier Microelectronics Reliability.

Francesco Iannuzzo received the MSc degree in Electronic Engineering and the PhD degree in Electronic and Information Engineering from the University of Naples, Italy, in 1997 and 2002, respectively. He is currently a professor of reliable power electronics at the Aalborg University, Denmark, where he is also part of CORPE, the Center of Reliable Power Electronics. His research interests are in the field of reliability of power devices, condition monitoring, failure modelling and testing up to megawatts under extreme conditions. He is author or co-author of about 300 publications on journals and international conferences, three book chapters and four patents, and has edited a book on Modern Power Electronic Devices (2020, IET). He is the co-founder of the Power Electronic Devices and Components journal, published by Elsevier. Besides the publication activity, over the past years he has been contributing about 30 technical seminars on reliability at top-tier conferences such as ISPSD, IRPS, EPE, ECCE, PCIM and APEC. Prof. Iannuzzo is currently the chair of the IEEE IAS Power Electronic Devices and Components Committee. In 2018 he was the general chair of the 29th ESREF, the first European conference on the reliability of electronics, and has recently been appointed general chair for the 2023 EPE-ECCE Europe conference in Aalborg.

Frede Blaabjerg (S'86–M'88–SM'97–F'03) was with ABB-Scandia, Randers, Denmark, from 1987 to 1988. From 1988 to 1992, he got the PhD degree in Electrical Engineering at Aalborg University in 1995. He became an Assistant Professor in 1992, an Associate Professor in 1996, and a Full Professor of power electronics and drives in 1998 at AAU Energy. From 2017 he became a Villum Investigator. He is honoris causa at University Politehnica Timisoara (UPT), Romania in 2017 and Tallinn Technical University (TTU), Estonia in 2018. His current research interests include power electronics and its applications such as in wind turbines, PV systems, reliability, Power-2-X, power quality and adjustable speed drives. He has published more than 600 journal papers in the fields of power electronics and its applications. He is the co-author of eight monographs and editor of fourteen books in power electronics and its applications. He has received 38 IEEE Prize Paper Awards, the IEEE PELS Distinguished Service Award in 2009, the EPE-PEMC Council Award in 2010, the IEEE William E. Newell Power Electronics Award 2014, the Villum Kann Rasmussen Research Award 2014, the Global Energy Prize in 2019 and the 2020 IEEE Edison Medal. He was the Editor-in-Chief of the IEEE TRANSACTIONS ON POWER ELECTRONICS from 2006 to 2012. He has been Distinguished Lecturer for the IEEE Power Electronics Society from 2005 to 2007 and for the IEEE Industry Applications Society from 2010 to 2011 as well as 2017 to 2018. In 2019–2020 he served as a President of IEEE Power Electronics Soc iety. He has been Vice-President of the Danish Academy of Technical Sciences. He is nominated in 2014–2021 by Thomson Reuters to be between the most 250 cited researchers in Engineering in the world.